

1 **An Excellent Full Sodium-Ion Capacitor Derived From a single**
2 **Ti-based Metal-Organic Frameworks**

3
4 Hao Chen, Chunlong Dai, Yanan Li, Renming Zhan, Minqiang Wang, Bingshu Guo, Youquan
5 Zhang, Heng Liu, Maowen Xu* and Shu-juan Bao*

6
7 Institute for Clean Energy & Advanced Materials, Faculty of Materials and Energy, Southwest
8 University, Chongqing 400715, P.R. China.

9
10 * Corresponding authors.

11 *E-mail* addresses: xumaowen@swu.edu.cn (M. W. Xu), baoshj@swu.edu.cn (S. J. B).

1. Experimental Section

Synthesis and characterization of TiO_xN_y : TiO_xN_y nanowires were obtained by annealing hydrogen titanate nanowires ($H_2Ti_3O_7$) in ammonia flow at 800 °C. $H_2Ti_3O_7$ NWs were firstly synthesized by hydrothermal method reported elsewhere.¹ Briefly, TiO_2 anatase (2 g) was added into NaOH solution (30 mL, 15 M) under magnetic stirring for 1 h. Then, the suspension was transferred to a Teflon-lined stainless steel autoclave and heated in an electric oven at 180 °C for 72 h. After cooling down at room temperature, the product was stirred in 0.1 M HCl solution for 24 h. The material was filtered, washed with deionized water and alcohol, and dried at 70 °C for 12 h. Finally, $H_2Ti_3O_7$ were converted to TiO_xN_y by annealing in NH_3 flow at 800 °C for 4 h with a heating rate of 5 °C min⁻¹.

2. Calculations of specific capacity, energy density and power density

The half-cell specific capacity (mAh g⁻¹) is calculated by **Equation S1**;

$$(1) \quad Q = i \times t$$

Q (mAh g⁻¹) is the half-cell specific capacity; i (mA g⁻¹) is the current density; t (h) is the charge or discharge time.

The Na-ion capacitors specific capacity (F g⁻¹), energy density (E) and power density (P) are calculated based on **Equations S2, S3 and S4**;

$$(2) \quad C = I \times \Delta t / (\Delta V)$$

$$(3) \quad E = (C \times \Delta V^2) / 2$$

$$(4) \quad P = E / \Delta t$$

32 C ($F\ g^{-1}$) is the Na-ion Capacitors specific capacity; I ($A\ g^{-1}$) is the current density; Δt (s) is the
 33 discharge time. ΔV is the charge-discharge potential window; E ($Wh\ kg^{-1}$) is the energy density and P
 34 ($W\ kg^{-1}$) is the power density.

35 **3. Calculate methods and details of capacitive effect contribution and diffusion-controlled** 36 **contribution**

37 Using the scan-rate-dependent CV curves (**Fig. 4A**) to quantify the contribution from capacitive
 38 effects (both surface pseudocapacitance and doublelayer capacitance) and diffusion-controlled Na^+
 39 insertion process to the current response according to the following equation;

$$40 \quad I(V) = k_1 v + k_2 v^{1/2}$$

41 Where I (V), $k_1 v$ and $k_2 v^{1/2}$ represent the total current response at a given potential V , current due to
 42 surface capacitive effects, and current due to diffusion-controlled Na^+ insertion process, respectively.

43 The above equation can also be reformulated as;

$$44 \quad I(V)/v^{1/2} = k_1 v^{1/2} + k_2$$

45 By plotting $I(V)/v^{1/2}$ vs. $v^{1/2}$ at different potentials, we can calculate the values of k_1 (slope) and k_2
 46 (intercept) from the straight lines. This allows one to quantify the fraction of the current at specific
 47 potentials to the capacitive effect ($k_1 v$) and diffusion-controlled insertion ($k_2 v^{1/2}$) at fixed potential (see
 48 **Fig. S13 A, B**). After integration of the enclosed CV area, the amount of stored charge from different
 49 energy storage modes can be distinguished, expressed by the following equation;

$$50 \quad Q = Q_s + Q_d$$

51 Where, Q , Q_s , and Q_d represent the total stored charge included in the enclosed CV area at set scan
 52 rate, surface capacitive effects, and diffusion controlled Na^+ insertion process, respectively.

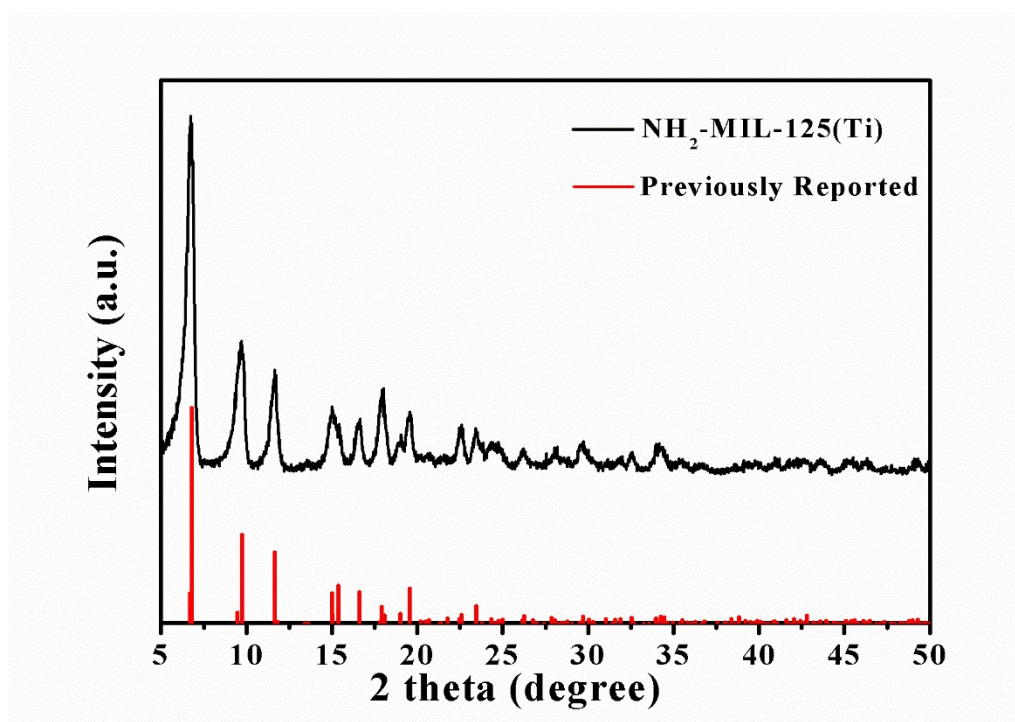


Fig. S1. XRD pattern of as-prepared $\text{NH}_2\text{-MIL-125(Ti)}$.

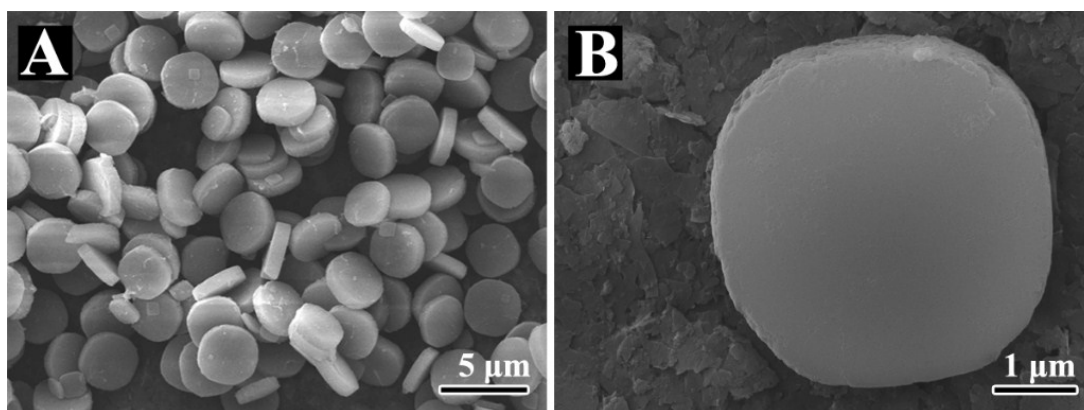


Fig. S2. (A and B) FESEM images of $\text{NH}_2\text{-MIL-125(Ti)}$ with different resolution.

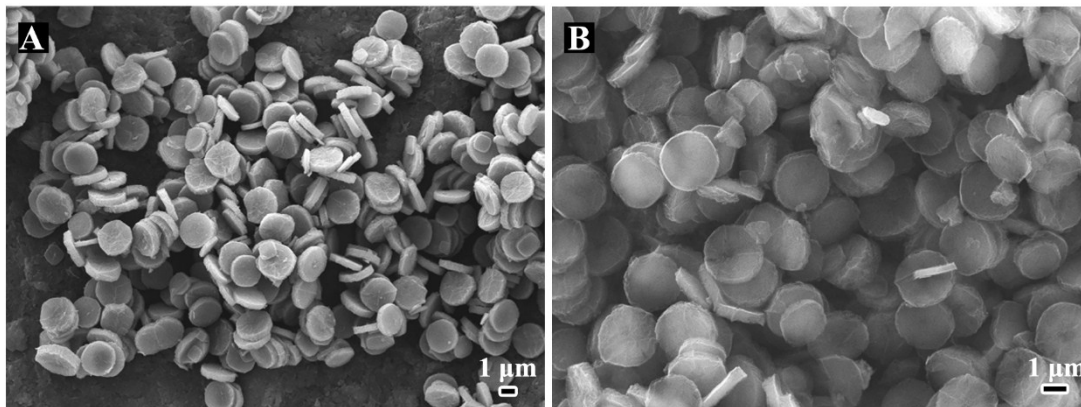


Fig. S3. (A and B) low resolution FESEM images of $\text{TiO}_x\text{N}_y/\text{C}$ and NHPC, respectively.

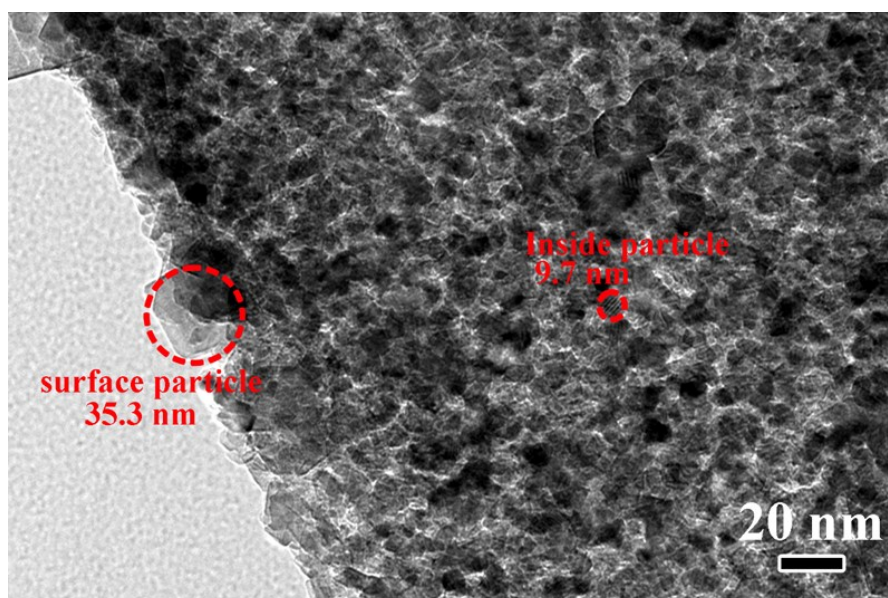


Fig. S4. bright-field TEM image of $\text{TiO}_x\text{N}_y/\text{C}$ inside structure.

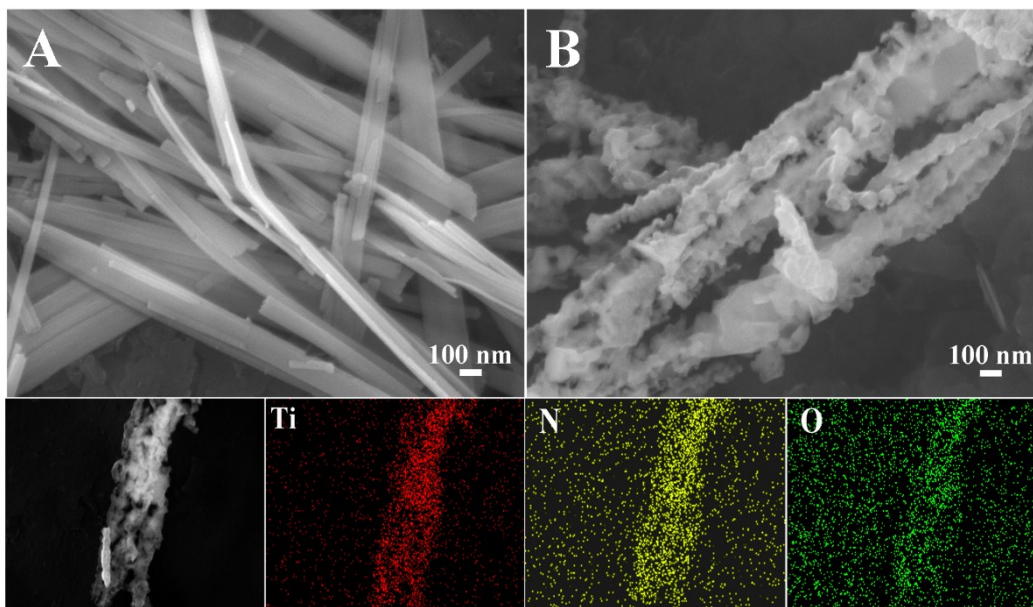


Fig. S5. (A) FESEM image of nanowires precursor, (B) FESEM image of TiO_xN_y nanowires and corresponding FESEM element mapping image.

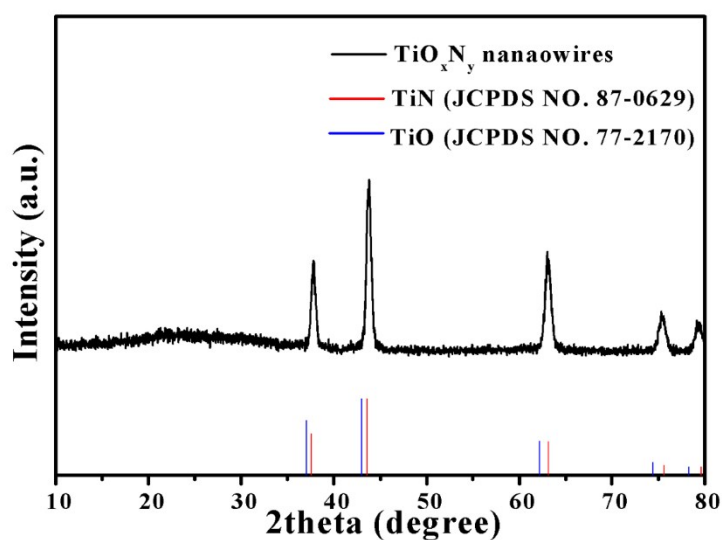
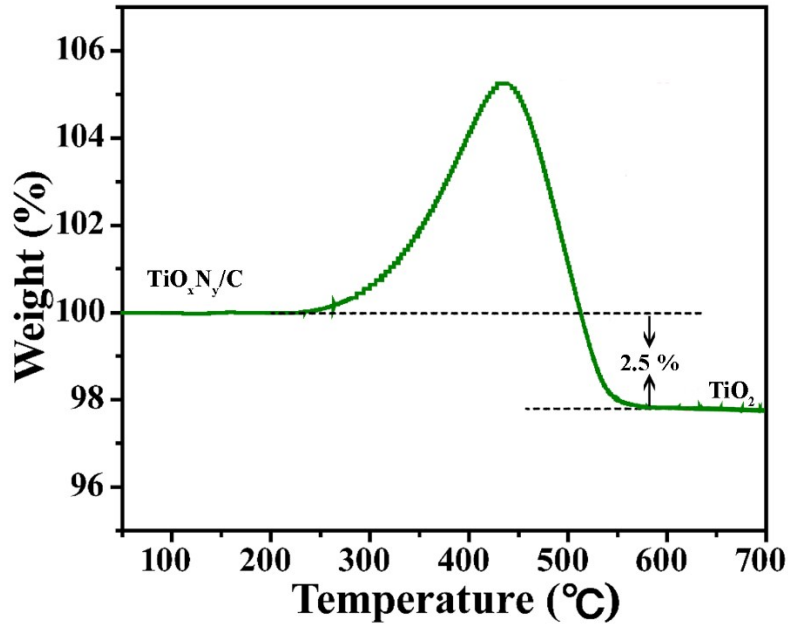


Fig. S6. XRD pattern of TiO_xN_y nanowires.



96

97 **Fig. S7.** Thermogravimetric analysis curves of $\text{TiO}_x\text{N}_y/\text{C}$.

98

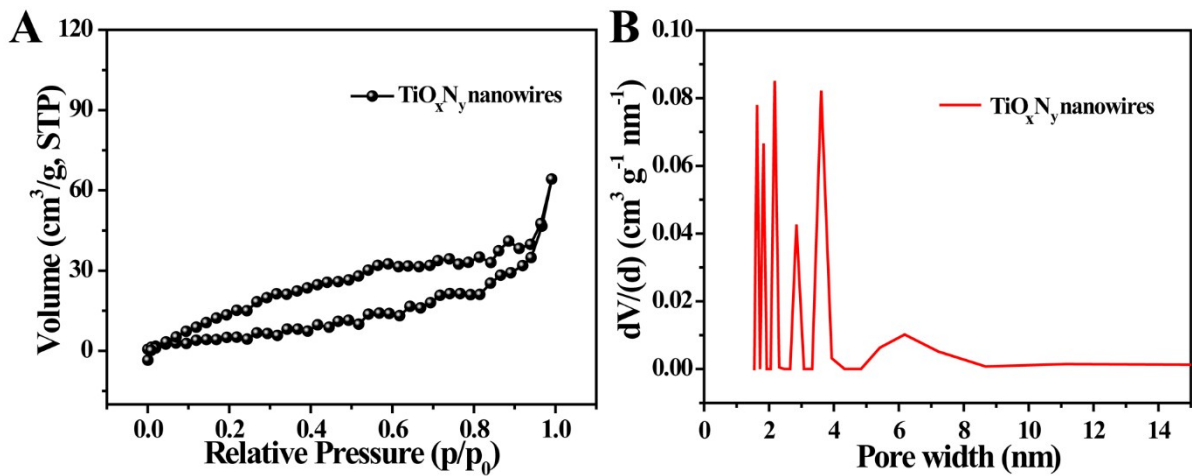
99 The TGA data was obtained by annealing in O_2 flow. In the detail, the original specimant is
 100 $\text{TiO}_x\text{N}_y(x+y=1)$ and carbon. The specimant converted to pure TiO_2 phase after TG test. So, according
 101 to the the finnal mass of TiO_2 and Invariance Principle of Ti elements in this process, the carbon
 102 contents in the $\text{TiO}_x\text{N}_y/\text{C}$ is approximately 22 % by calculated.

103

104

105

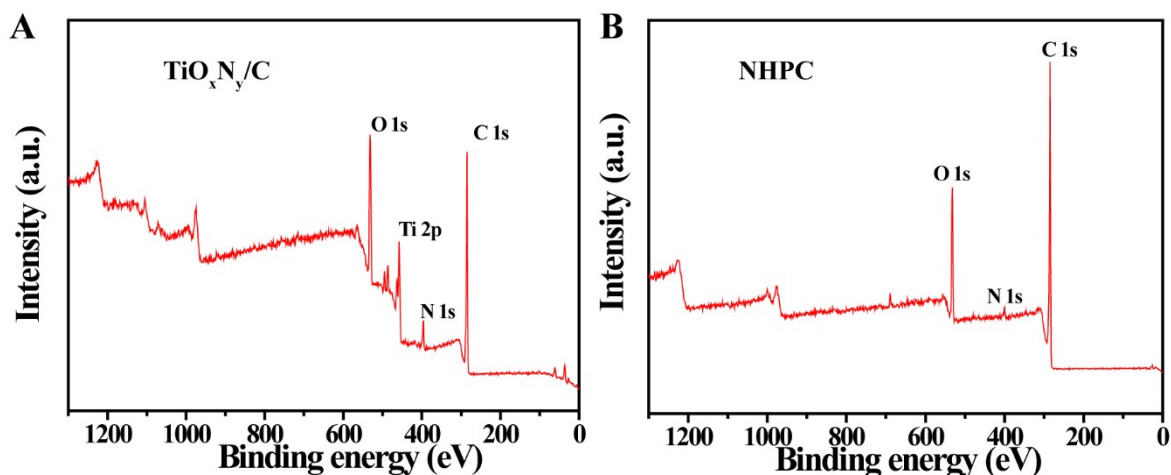
106



107

108 **Fig. S8.** (A) The nitrogen adsorption-desorption isotherms of TiO_xN_y , and (B) the corresponding pore
 109 distribution.

110



111

112

113 **Fig. S9.** (A and B) XPS spectra of $\text{TiO}_x\text{N}_y/\text{C}$ and NHPC, respectively.

114

115

116

117

118

119

120

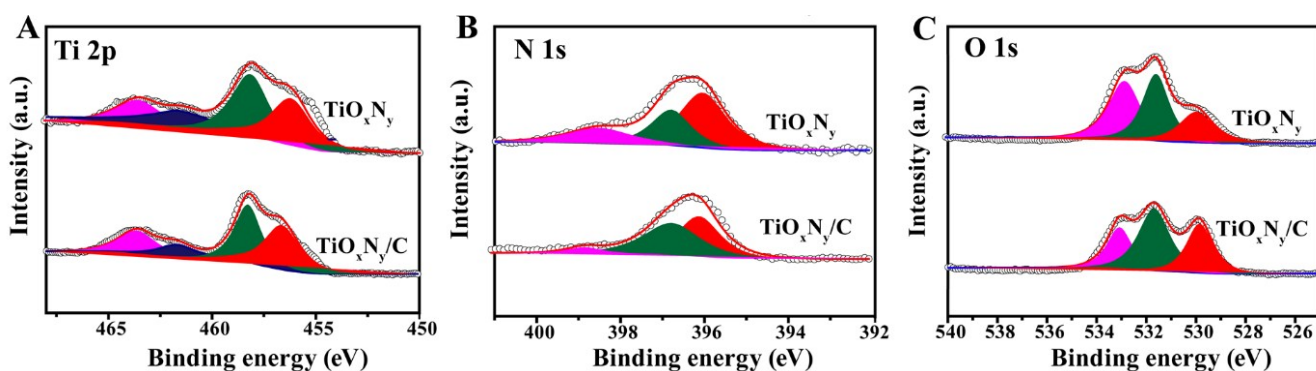
121

122

123

124

125



126

127 **Fig. S10.** (A, B and C) the contrast of Ti 2p, N 1s and O 1s XPS spectra between $\text{TiO}_x\text{N}_y/\text{C}$ and
128 TiO_xN_y nanowires, respectively.

129

130

131

132

133

Sample	Textural properties	
	$S_{\text{BET}}^{\text{a}}(\text{m}^2\text{g}^{-1})$	$V_{\text{t}}^{\text{b}}(\text{cm}^3\text{g}^{-1})$
C	1731	1.12
$\text{TiO}_x\text{N}_y/\text{C}$	248	0.5
TiO_xN_y	20.921	0.11

Table S1. the structure information of as-prepared samples.

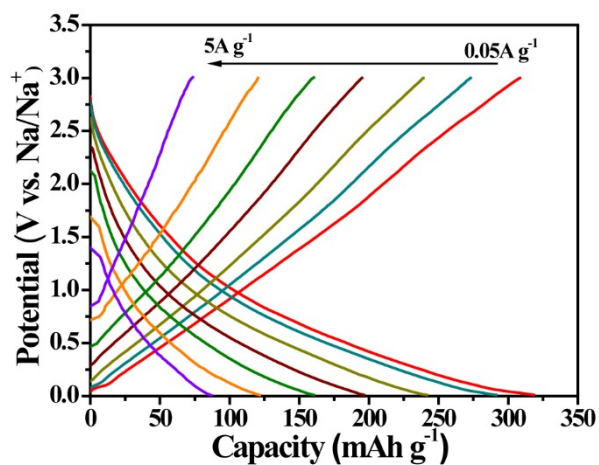


Fig. S11. Charge and discharge curves of $\text{TiO}_x\text{N}_y/\text{C}$ at different current density.

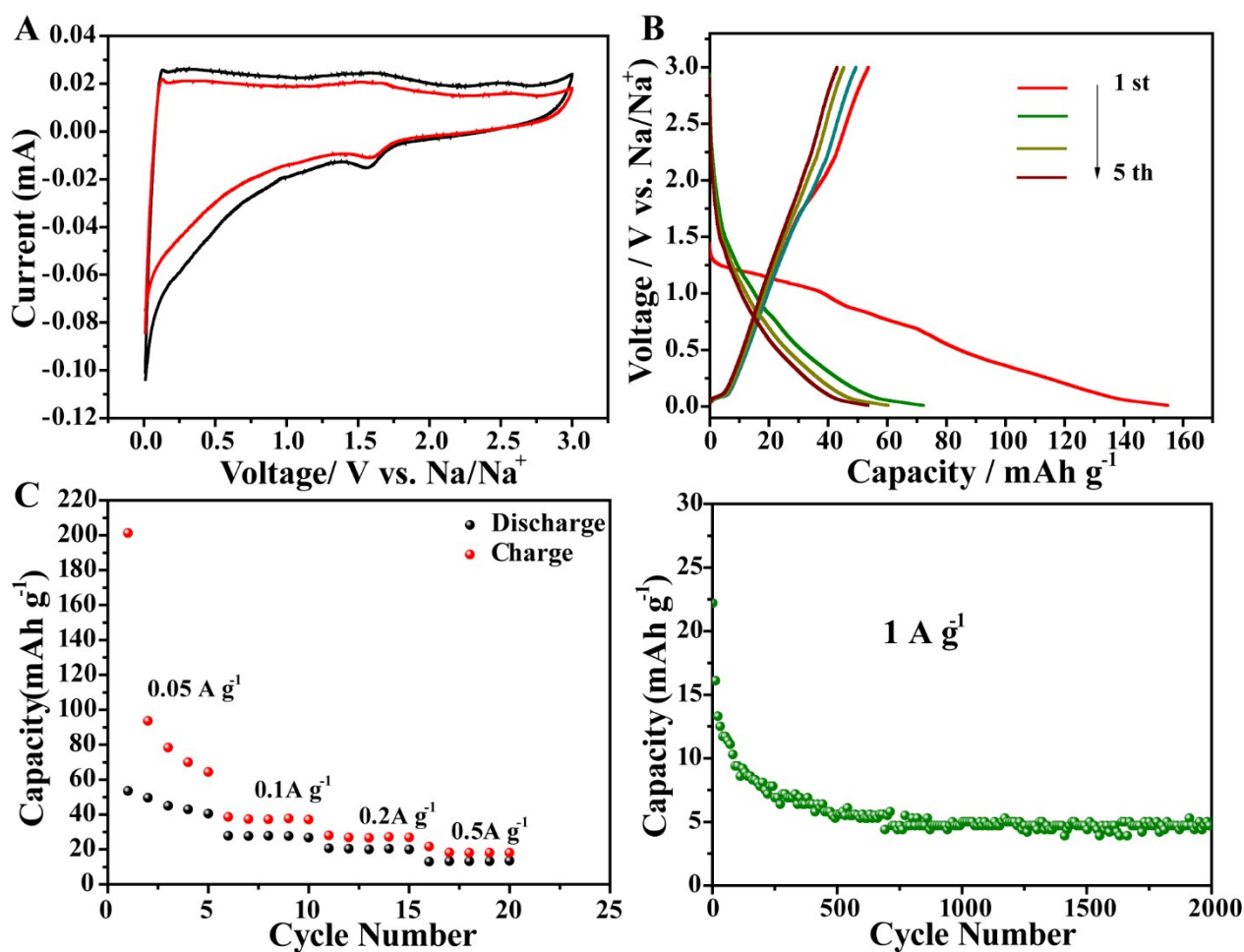


Fig. S12. CV curves (A), first five galvanostatic discharge–charge profiles at 0.05 A g^{-1} (B), rate performance (C) and the cycling stability of at 1 A g^{-1} of TiO_xN_y nanowires.

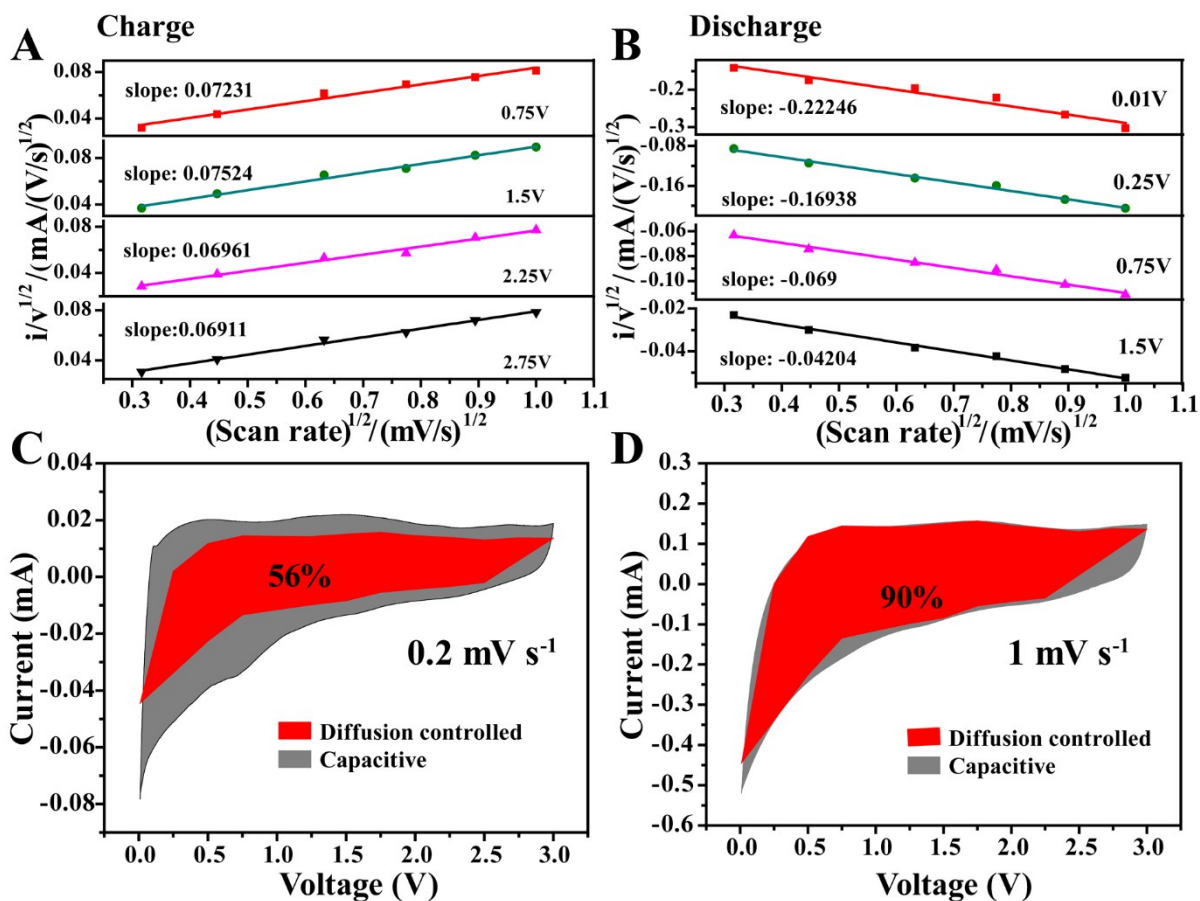


Fig. S13. (A and B) $I/v^{1/2}$ vs. $v^{1/2}$ plots of $\text{TiO}_x\text{N}_y/\text{C}$ used for calculating constants k_1 and k_2 at different potentials, (C and D) Capacitive charge storage contributions at a scan rate of 0.2 mV s^{-1} and 1 mV s^{-1} .

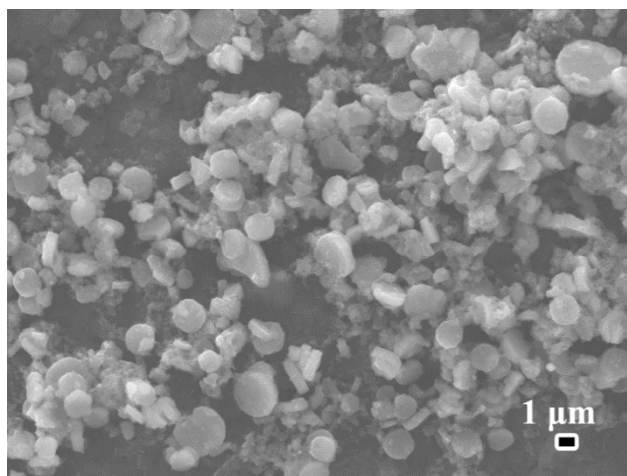


Fig. S14. FESEM images of $\text{TiO}_x\text{N}_y/\text{C}$ after electrochemical cycles test.

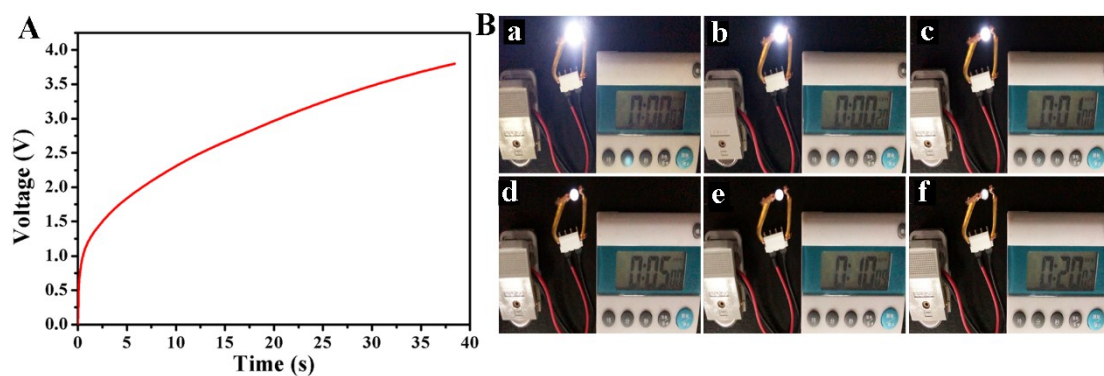


Fig. S15. The rapid charging curves in 40s of $\text{TiO}_x\text{N}_y/\text{C} // \text{NHPC}$ SICs (B), and the Photographs of a light emitting diode powered by a rapid charging $\text{TiO}_x\text{N}_y/\text{C} // \text{NHPC}$ SIC in 40 s under time recording by a timer.